Numerical Study for the Performance Analysis and Design of a Crossflow-Type Forced Draft Cooling Tower

Young Ki Choi**, Byung Jo Kim*, Sang Yun Lee*, Jung Hee Lee*

Key words : Heat and mass transfer, Cooling tower, Crossflow, Forced draft, Turbulent 2-phase flow, Standard k-ε model, Finite volume method, Non-orthogonal grid system

Abstract

A numerical study for performance analysis of a crossflow-type forced draft cooling tower has been performed based on the finite volume method with non-orthogonal body fitted, and non-staggered grid system. For solving the coupling problem between water and air, air enthalpy, moisture fraction, water enthalpy, and water mass balance equations are solved with Navier-Stoke's equations simultaneously. For the effect of turbulence, the standard k-ε turbulent model is implied in this analysis. The predicted result of the present analysis is compared with the experimental data and the commercial software result to validate the present study. The predicted results show good agreement with the experimental data and the commercial software result. To investigate the influence of the cooling tower design parameters such as approach, range and wet bulb temperature, parametric studies are also performed.

Nomenclature

a : area of transfer surface per unit volume [㎡/㎥]

A : control surface [㎡]

c_{pl} : constant pressure specific heat of water [J/kg · K]

C_μ , C_1 , C_2 : standard k-ε turbulence model constant

D : diffusion conductance

f_x : resistance to air flow in x direction [N/㎥]

f_y : resistance to air flow in y direction [N/㎥]

* Graduate School, Chung-Ang University, Seoul 156-756, Korea
** Department of Mechanical Engineering, Chung- Ang University, Seoul 156-756, Korea

f_G : moisture fraction in air [kg/kg]
g : gravitational acceleration [m/s^2]
G : air mass flow rate [kg/s]
h : enthalpy [J/kg]
k : turbulent kinetic energy [㎡/S^2]
K : mass transfer coefficient[kg/㎡s]
L : water mass flow rate[kg/s]
m : mass of water vapor or liquid[kg]
n : empirical constant for fill
N : number of velocity head loss
P : pressure [Pa]
P_e : Peclet number of east node point
$\dot{q}$: rate of heat transfer [W]
R : universal gas constant [J/kg · mol · K]
t : temperature of water [℃]
V : control volume [㎥]
x, r : cylindrical coordinates
x^i : non-orthogonal coordinates
y^i : Cartesian coordinates
u, v : Cartesian velocity components in the y^1, y^2 directions
w : absolute humidity[kg/kg]

Greek symbols

α : Cartesian component of the contravariant base vector
Γ : diffusion coefficient
δ : Kronecker's delta
ε : dissipation rate of turbulent kinetic energy
λ : empirical constant for fill
μ : viscosity [kg/m·s]
ν : specific volume [㎥/kg]
ρ : density [kg/㎥]
σ : Prandtl number
ϕ : dependent variable

Subscripts

1 : inlet port
2 : outlet port
amb : ambient
avg : average
DB : dry bulb
eff : effective
elim : eliminator
F : water
G : moist air
S : saturated
WB : wet bulb

1. Introduction

Cooling towers are often used in industrial air-conditioning systems and heat exchangers to get rid of the wasted heat. Today, the demand for a cooling tower is increasing with the promotion and distribution of refrigerating and air-conditioning industry. This calls for the technical accumulation for the optimal design of cooling towers. Apparatus for the actual design process must be set up for each experiment according to their tower type, shape, fill, etc. and it is very economically and timely unfavorable to satisfy other external operating conditions. In order to make up for these defects, analysis methods to proficiently gather data for each set of conditions by numerically devising cooling towers which run under the given operating conditions are taken into consideration.

The theory about the operation of cooling tower was first proposed by Walker[1] but Merkel[2] was the first one to apply the differential equations to its analysis. Merkel assumed Lewis number to be 1 for air-water systems and presented heat transfer rate in the cooling tower as a function proportional to the difference between the saturated air enthalpy and the mean enthalpy of local air. This equation has so far been used for the calculation of the cooling tower performance. Lichtenstein[3] managed to find a graphical solution using the Merkel's equation. Baker and Shryock[4] reinspected the Merkel's research and tried to minimize the errors found in the Merkel's assumptions. The Cooling Tower Institute developed the cooling tower design curve[5] based on the Merkel's theory. Majumdar, etc.[6] applied FDM on the governing 2-D partial differential equation of fluid flow and heat and mass transfer in the cooling tower and developed VERA2D; a commercial program for analyzing fluid flow and heat transfer phenomenon in a cooling tower. This program was applied to cooling towers of simple type using the orthogonal coordinates and linear turbulent models[6,7] using the characteristic lengths.

This study consists of a numerical analysis on the general crossflow forced draft cooling towers. First of all, water vapor loss due to its evaporation in the cooing tower and the coupling between air and water are put into consideration and 2-D symmetric turbulent two-phase flow equations are solved using the Finite Volume Method based on the non-orthogonal coordinate system. The standard $k-\varepsilon$ turbulent model is chosen to take effects of turbulence into consideration. To verify the validity of these results, they are compared with the experimental and the commercial program results. The effects of the flow variations in the tower on the cooling tower performance and the effects of operating condition variations on its efficiency, capacity, range and approach are also examined.

2. Main

The basic concept of this study is to separate the analysis domain into air and water domains. The governing equations for each domain are developed and solved using the finite volume method. The following assumptions and models are suggested to simplify the governing equations. The analyses are made for counterflow and crossflow forced draft cooling towers, respectively.

2.1 Assumptions

The assumptions for governing equations are as follows.[4]

- Heat and mass transfer occurs in the air water interface.
- Air is saturated in the air-water interface.
- There is no resistance in mass transfer process.
- Temperature gradient is zero at the interface.
- Heat and mass diffusion coefficients are the same for air-water system.
- Only parallel direction to the flow is considered for heat and mass transfer of water.

2.2 Governing equations

2.2.1 Air

The mass equilibrium equation is

$$\frac{1}{J}\frac{\partial}{\partial x^j}\left[Ja^j_m(\rho U_m)\right] = \dot{m}_v''' \qquad (1)$$

The momentum equilibrium equation is

$$\frac{1}{J}\frac{\partial}{\partial x^j}\left[Ja^j_m(\rho U_m U_i - \tau_{mi} + P\delta_{mi})\right] = -f_i - (\rho - \rho_{amb})g\delta_{1i} \quad (2)$$

Referring to the Equation(2), τ_{mi} presents the viscous stress and the Reynolds stress introduced by time-averaging momentum equation for turbulent flow: that is,

$$\tau_{mi} = \mu_{eff}\left[\frac{\partial U_i}{\partial x^n}a^n_m + \frac{\partial U_m}{\partial x^i}a^l_i\right] - \frac{2}{3}\delta_{mi}k \quad (3)$$

where μ_{eff} presents the isotropic effective viscous coefficient defined as the combination of turbulent viscous coefficient(μ_t) and molecular viscous coefficient(μ), and turbulent viscous coefficient(μ_t) can be written as

$$\mu_t = \rho C_\mu \frac{k^2}{\varepsilon} \quad (4)$$

The turbulent energy transport equation is

$$\frac{1}{J}\frac{\partial}{\partial x^j}\left[Ja^j_m\left(\rho U_m k - \frac{\mu_t}{\sigma_k}\frac{\partial k}{\partial x^n}a^n_m\right)\right] = P_k - \rho\varepsilon \quad (5)$$

The turbulent energy dissipation rate equation is

$$\frac{1}{J}\frac{\partial}{\partial x^j}\left[Ja^j_m\left(\rho U_m \varepsilon - \frac{\mu_t}{\sigma_\varepsilon}\frac{\partial \varepsilon}{\partial x^n}a^n_m\right)\right] = \frac{\varepsilon}{k}(C_1 P_k - C_2\rho\varepsilon) \quad (6)$$

where σ_k and σ_ε are the diffusion turbulent Prandtl numbers for the $k-\varepsilon$ model. C_μ, C_1, C_2 are the general $k-\varepsilon$ turbulent model constants. P_k is defined in terms of the source of turbulent energy as

$$P_k = \mu_t\left[\frac{\partial U_i}{\partial x^n}a^n_j + \frac{\partial U_j}{\partial x^m}a^m_i\right]\left[\frac{\partial U_i}{\partial x^n}a^n_j\right] \quad (7)$$

The enthalpy equilibrium equation is

$$\frac{1}{J}\frac{\partial}{\partial x^j}\left[Ja^j_m\left(\rho U_m h_G - \Gamma_{eff}\frac{\partial h_G}{\partial x^n}a^n_m\right)\right] = \dot{q}''' \quad (8)$$

The moisture equilibrium equation is

$$\frac{1}{J}\frac{\partial}{\partial x^j}\left[Ja^j_m\left(\rho U_m f_G - \Gamma_{eff}\frac{\partial f_G}{\partial x^n}a^n_m\right)\right] = \dot{m}_v \quad (9)$$

where Γ_{eff} is the effective heat diffusion coefficient which includes molecular heat diffusion and defined in the following form

$$\Gamma_{eff} = \frac{\mu}{\mathrm{Pr}} + \frac{\mu_t}{\mathrm{Pr}_t} \quad (10)$$

2.2.2 Water

The mass equilibrium equation is

$$\frac{1}{J}\frac{\partial}{\partial x^1}\left[Ja^1_1(\rho_F U_F)\right] = -\dot{m}_v''' \quad (11)$$

The enthalpy equilibrium equation is

$$\frac{1}{J}\frac{\partial}{\partial x^1}\left[Ja^1_1(\rho_F U_F h_F)\right] = -\dot{q}''' \quad (12)$$

where U_m and U_F, described above, represent Cartesian velocity components for air and water, respectively. y_i is a Cartesian coordinate and x^j is a general coordinate. J represents Jacobian x^j by the transformation into a non-orthogonal coordinate and can be expressed as

$$J = det\left|\frac{\partial(y_1, y_2)}{\partial(x^1, x^2)}\right| \quad (13)$$

where a^j_m represents the inner products of a non-orthogonal coordinate contravariant base vector, e^j and a Cartesian vector, i_m, and δ_{mi} represents the Kronecker's delta.

2.2.3 Models for resistance to air-flow and for heat and mass transfer.

A model for resistance to air-flow

The air flow resistances offered by various solid obstacles within the tower are expressed in the following integrated form[6],

$$\int f_x dV = N\frac{1}{2}\rho u^2 \Delta V + N_{louver}\frac{1}{2}\rho u^2 \Delta A + N_{elim}\frac{1}{2}\rho u^2 \Delta A \quad (14a)$$

$$\int f_y dV = N\frac{1}{2}\rho v^2 \Delta V + N_{louver}\frac{1}{2}\rho v^2 \Delta A + N_{elim}\frac{1}{2}\rho v^2 \Delta A \quad (14b)$$

where ΔV is the control volume and ΔA is the area of the control cell face normal to the velocity component. N is the number of velocity heads loss per unit air travel distance in the fill. N_{louver} and N_{elim} are the total number of velocity head losses in the louver and eliminator, respectively. N is expressed by Kelly[8] in the following form.

$$N = \lambda_v \frac{L''}{G''} + n_v \quad (15)$$

where λ_v and n_v are empirical constants.

A model for heat and mass transfer

Rates of heat transfer and mass transfer per unit volume are based on the use of Merkel's equation[6], which is

$$\dot{q}''' = Ka(h_S - h_G) \quad (16)$$

$$\dot{m}_v''' = Ka(f_S - f_G) \quad (17)$$

where K is the mass transfer coefficient and a is the area of contact surface of water and air per unit volume. Ka can be calculated by using the empirical formulations of Kelly[8] in the following form,

$$\frac{Ka}{L''} = \lambda_h \left(\frac{L''}{G''}\right)^{-n_h} \quad (18)$$

where λ_h and n_h are the empirical constants.

2.2.4 Flow property equations

The density of air can be calculated by employing the following equation of the state

$$\rho = \frac{PW_G}{R(T_{db} + 273.15)} \quad (19)$$

where R is the universal gas constant, and W_G is the molecular weight of moist air and can be calculated in the following form

$$W_G = W_{air}(1 - f_G) + W_{water} f_G \quad (20)$$

where W_{air} is the molecular weight of dry air and W_{water} is the molecular weight of water.

The moisture fraction(f_S) and enthalpy(h_S) in the air of saturation state are required for calculating heat and mass transfer. The moisture fraction($f_{G,amb}$) and enthalpy($h_{G,amb}$) of inlet air are used as the boundary condition of the enthalpy equilibrium equation and the moisture fraction equilibrium equation. The PROPATH[9] function is employed for the calculation of f_S, h_S, $f_{G,amb}$, $h_{G,amb}$, and dry bulb temperature of air.

2.3 Boundary conditions

2.3.1 The inlet boundary conditions

The enthalpy and moisture fraction of inlet air are calculated by employing PROPATH[9] function with the given ambient dry-bulb temperature, wet-bulb temperature, and pressure.

2.3.2 The outlet boundary conditions

The outlet mass flux is handled to equal the sum of inlet mass and evaporated mass to satisfy the overall continuity equation in calculating domains.

2.3.3 The symmetric boundary conditions

The value of normal gradient at symmetric boundary plane of all dependent variables is taken as zero.

2.3.4 Wall boundary conditions

No-slip condition is taken into consideration at the velocity field, and the other scalar variables are taken to be adiabatic. It is illogical that the temperature of wall is isothermal because the distribution of wall temperature is different during, in reality, the process of thermal exchange within the tower. Due to this reason, the condition of isothermal wall is not applied. Beyond these, the source term is handled to express resistances to air-flow of a fill and an eliminator in the air-momentum equilibrium equation within the air domain, heat transfer between air and water in the enthalpy equilibrium equation of air and water, and mass transfer in the moisture fraction equation of air and water, respectively. The source term is also handled to consider the mass balance according to the mass transfer in the pressure equation which includes the mass equilibrium equation.

2.4 Numerical analysis

2.4.1 The shape and components of a cooling tower

The shape of a cooling tower uses materials of references[10,11]. The schematic shape and components are shown in Fig. 1. The detailed shape specifications of the cooling tower is shown in Table 1.

Table 1 The specifications of the cooling tower

Mean half-width of the tower	9.70
Longitudinal width of the cell	10.97
Cell height	11.98
Air travel width of the fill	5.18
Inclined angle of the inlet louver	8°
Fan diameter	8.53
Hub diameter	1.22
Stack diameter	9.68
Stack height	4.27
	unit except inclined angle:[m]

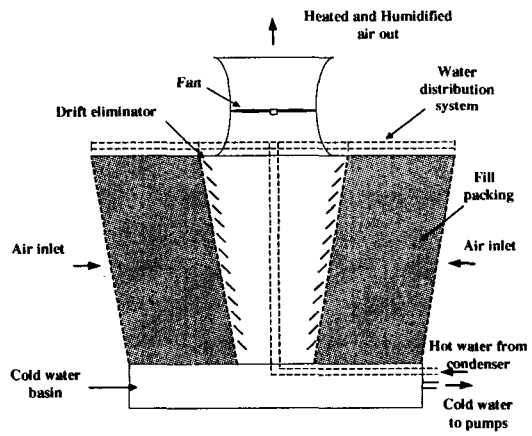

Fig. 1 Forced draft crossflow tower.

2.4.2 Grid arrangements

For boundary grid nodes, the distribution function is used in treating curves and the distance of grid line. For inner grid nodes, interpolation is used in conjunction with the ratio of the outer grid arrangements. The grid system used in this study is a two-dimen-

sional symmetric non-orthogonal coordinate. The nonuniform non-staggered grid system 101 ×99 into the directions of x, y is used. Figure 2 depicts the grid system.

2.4.3 The discretization of governing equations

The algebraic equations are obtained by using the finite-volume method to integrate the previously derived governing equations over a control volume. During the discretization process, the power-law scheme is used in the convective term, the central difference scheme in the normal diffusion term, and the harmonic average in the cross diffusion term.

2.4.4 The analytic method

Each discretization equations are calculated by using the SIP(Strongly-Implicit Procedure) method, and the SIMPLE algorithm is used to calculate the pressure field. Considering a non-staggered grid, the velocity components at the control surface should be calculated by interpolation to obtain the pressure correlation equation. The Modified Rhie's method[12] is used for pressure-velocity coupling for the non-staggered grid.

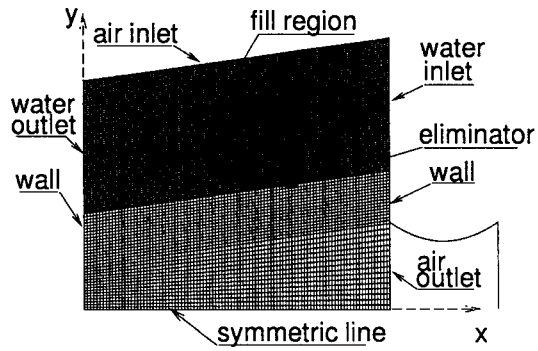

Fig. 2 Grid system and boundary conditions for the crossflow type tower.

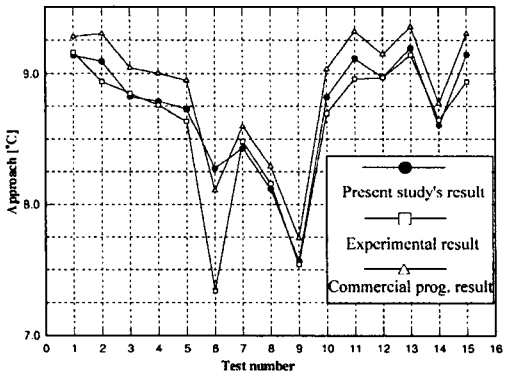

Fig. 3 Comparison of present result with experimental and commercial program result.

3. Results and Investigation

Heat and mass transfer is analyzed by the numerical analysis for the forced draft crossflow cooling tower. First, these data are compared with the experimental data of reference[10] to verify the validity of this analysis.

3.1 The verification of programming

The analysis of the cooling tower is carried out according to the following operating condition for the forced draft crossflow. Tables 1 and 2 present the shape specifications and operating conditions used in an experiment and an analysis. The wedged plastic airfoil type fill is used. Figure 3 presents each approach for experimental results, commercial program results, and present study's results for each operating condition. Generally, the results of analysis match well with the results of experiment.

3.2 The analysis for forced draft crossflow type cooling towers

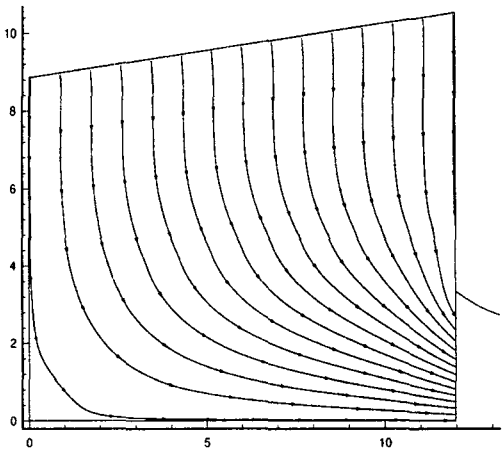

Fig. 4 Streamline in a crossflow type tower.

Table 4 Calculation result for the forced draft crossflow tower

Average water outlet temperature[℃]	30.97
Range[℃]	8.02
Approach[℃]	8.81
Cooling tower effectiveness	0.48

The shape specifications and operating conditions are shown in Tables 1 and 3, respectively. The plastic airfoil type H fill is used. According to the conditions presented above, the symmetric 2-D steady state fluid flow is analyzed. The final results are shown in Table 4. Maximum residual was set less than 10^{-3} as the converging condition. For each equilibrium equation, the computing time was about 12 minute using the Intel Pentium II 266 MHz PC.

Figure 4 shows the streamline distribution in the tower. Circulation does not occur at the air entrance. In the case of the counterflow type, the air passing by the entrance changes the flow direction abruptly but there is the same main flow direction in the air entrance and the fill region of the crossflow type.

Figure 5 shows the pressure distribution. Pressure decreases along the air progressing direction due to flow resistance in the fill.

Figure 6 shows the x-directional velocity component distribution. Like the counterflow, the velocity decreases due to flow resistance

Table 2 Operating conditions for the field test data

Test number	Operating conditions (Air mass flow rate:644kg/s)			
	Range [℃]	Dry bulb temp.[℃]	Wet bulb temp.[℃]	Water mass flow rate[kg/s]
1	8.33	29.00	21.38	1118.25
2	8.29	29.80	21.87	1148.57
3	8.10	30.25	22.25	1153.68
4	8.11	30.30	22.28	1148.96
5	8.06	30.50	22.39	1152.51
6	7.78	32.00	22.85	1143.45
7	7.73	30.25	22.26	1132.82
8	7.56	31.00	22.67	1130.46
9	7.31	31.80	23.56	1126.52
10	8.02	30.15	22.16	1155.66
11	8.20	29.55	21.75	1153.29
12	8.09	29.45	21.66	1137.94
13	8.15	28.85	21.26	1137.94
14	7.79	30.00	22.02	1137.94
15	8.11	28.95	21.31	1137.94

Table 3 Operating conditions for the present study

Wet bulb temperature[℃]	22.16
Dry bulb temperature[℃]	30.15
Ambient pressure[kPa]	101.325
Inlet water temperature[℃]	40.00
Water mass flow rate[kg/s]	1155.66
Air mass flow rate[kg/s]	644.0

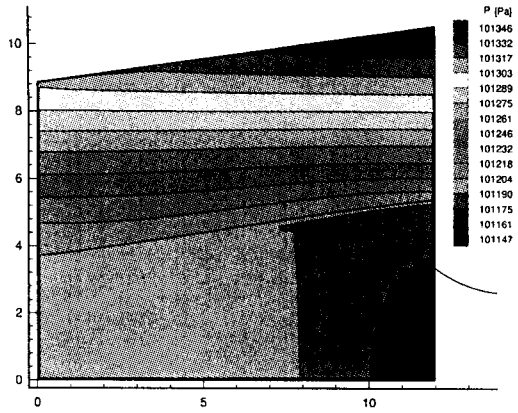

Fig. 5 Isobaric contour in a crossflow typ tower.

near the fill, also near the eliminator, and the recovery of velocity is perceptible in the exit direction.

Figure 7 shows the air temperature field. The lower temperature distribution is shown along the direction toward the air entrance and the cooling water exit. Figure 8 shows the water temperature field. The variation of temperature near the sprayer is small along the air-progressing direction but abrupt temperature variation is shown in this direction. This is due to the increase of heat exchange time between air and water, which approach the cooling water exit. Temperature distribution corresponds to air temperature distribution of Fig.7.

Various operating conditions were considered to find out the optimal operating condition data. Figure 9 shows the influence of inlet water temperature along the water mass flow rate, when the dry-bulb temperature of entrance air is fixed as 30.15℃, wet-bulb temperature as 22.16℃, and air mass flow rate as 800 kg/s. Figure 9-a presents the range. The less water mass flow rate is getting, the more range increases. The higher water entrance temperature is, the more amount of increase, namely

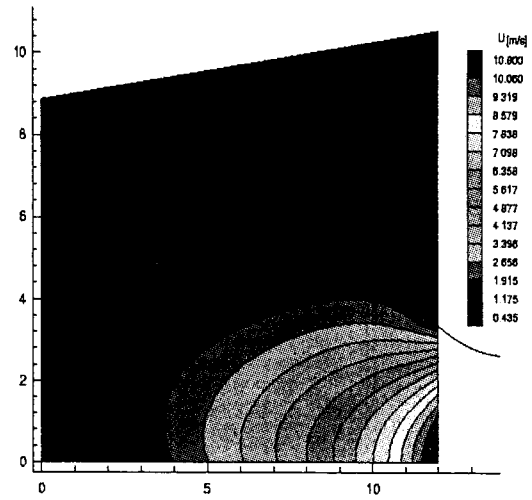

Fig. 6 U velocity contour in a crossflow type tower.

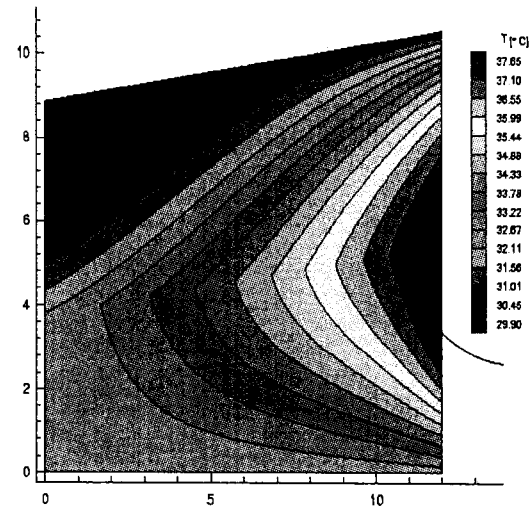

Fig. 7 Isothermal contour in a crossflow type tower.

the temperature difference between air and water, is getting. Figure 9-b presents the total cooling capacity. The higher water entrance temperature is, the more the amount of cooling capacity is getting due to the increase of water mass flow rate. That is why the increase of range due to the increase of water entrance

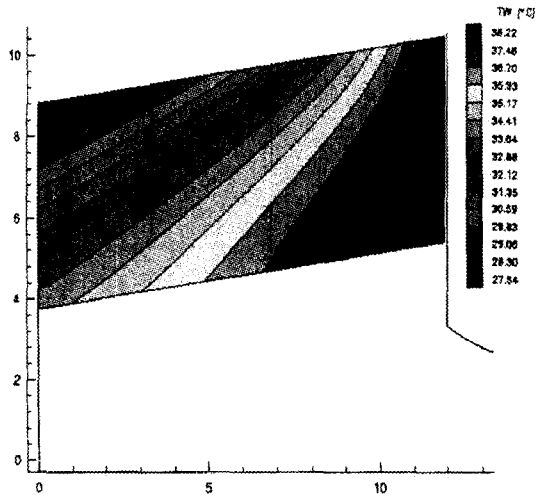

Fig. 8 Water isothermal contour in a crossflow type tower.

temperature exceeds the decrease of range due to the increase of water mass flow rate. Figure 9-c presents the variation of approach. The less water mass flow rate is and the lower water entrance temperature is, the lower approach is. The water mass flow rate is dominant as water entrance temperature is getting higher. Figure 9-d presents the effectiveness of the cooling tower. The effectiveness presents the cooling capacity of the given operating conditions in the ratio of the difference between water entrance temperature and wet-bulb temperature of entrance air to range. The more water mass flow rate is, the worse cooling effectiveness is and the higher water entrance

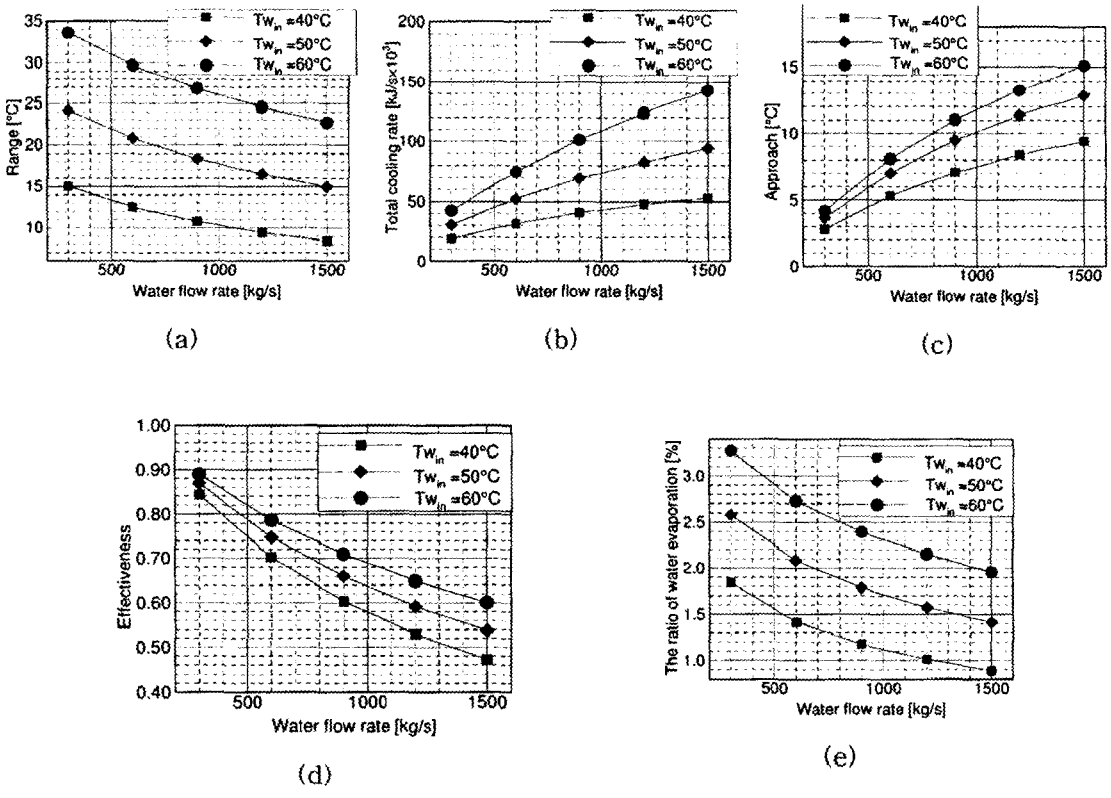

Fig. 9 The effect of inlet water temperature on water mass flow rate.

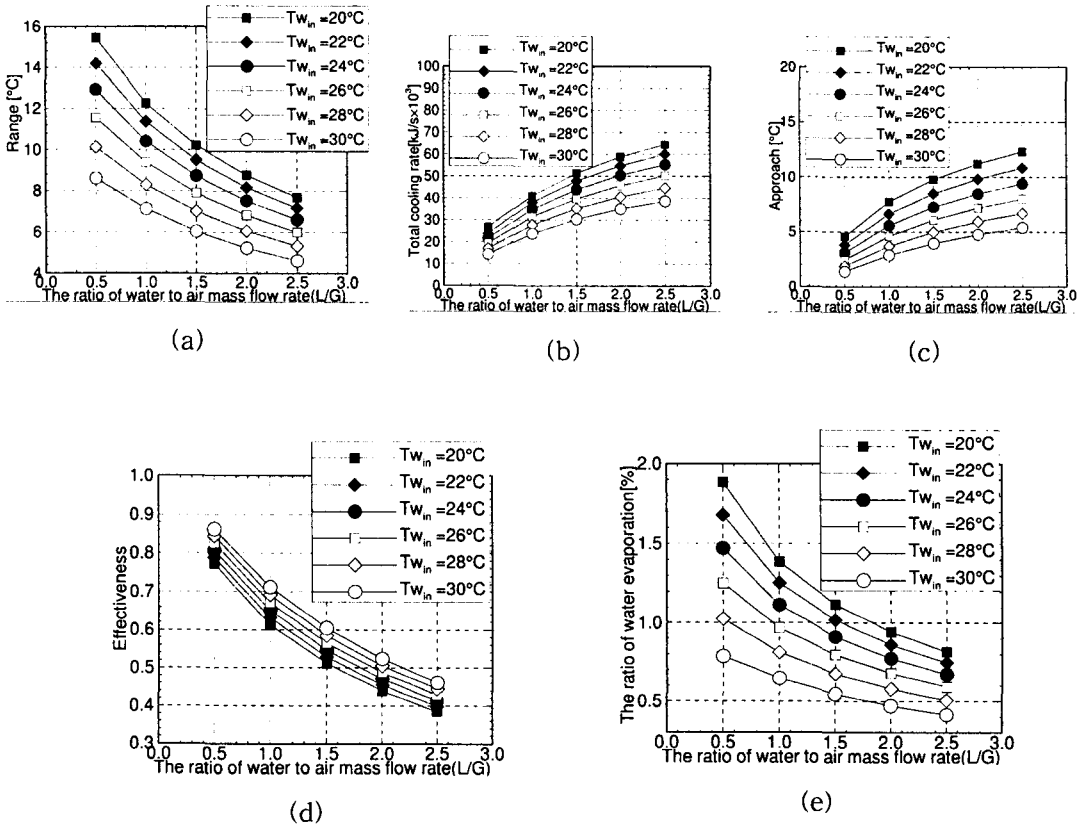

Fig. 10 The effect of inlet wet temperature on L/G.

temperature is, the better cooling effectiveness is. Water mass flow rate has also much influence on the effectiveness. Figure 9-e presents the percent of water evaporation. According to the increase of water mass flow rate, absolute evaporation increases but relative amount decreases.

Figure 10 shows the influence of air wet-bulb temperature according to the mass flow rate ratio of water over air, when water entrance temperature is fixed as 40℃ and air dry-bulb temperature as 30.15℃. Figure 10-a presents the range. The lower mass flow rate ratio and wet-bulb temperature are, the more range increases: that is, the lower relative humidity is, the more range increases. The range increases as mass flow rate ratio is getting low and interface time between air and water increases. When the wet-bulb temperature is low, the increase of range is shown to be abrupt according to the decrease of mass flow rate ratio. This is due to heat exchange by evaporation as wet-bulb temperature is low. Figure 10-b presents the total cooling capacity. This increases according to the decrease of wet-bulb temperature. That is why the range decreases as the mass flow rate ratio is getting higher. Figure 10-c shows that the lower mass flow rate ratio is and the higher wet- bulb temperature, the lower approach is. As the wet-bulb

temperature is low, the variation of mass flow rate ratio has much influence on the approach. Figure 10-d shows that as the wet-bulb temperature is getting higher, the effectiveness of the cooling tower increases but is not much influenced. On the contrary, this increases very much, as the mass flow rate ratio decreases. Hence the mass flow rate ratio has much influence on the effectiveness. Figure 10-e presents the percent of water evaporation. This shows the similar curve distribution with the range. As the mass flow rate ratio is low in low wet-bulb temperature, evaporation increases very much. It is shown that the mass flow rate ratio has much influence on evaporation. The variation of mass flow rate ratio has sensitive influence on the capacity of the cooling tower, especially for the case of good operating conditions; that is, low wet-bulb temperature and high dry-bulb temperature.

4. Conclusions

In this study, through the analysis of flow field in the forced draft crossflow cooling towers, the basic data for evaluation of the cooling tower performance were acquired. The following results were also obtained.

(1) Two phase flow in the cooling tower was analyzed with water vapor loss and air-water coupling in consideration. The standard $k-\varepsilon$ model was chosen and turbulent effects were also considered. Properties to evaluate the flow types, temperature distribution and cooling performance for various tower shapes and operating conditions were predicted. The predicted results matched well with the experimental and commercial program results.[10]

(2) Under the better operating conditions such as lower wet bulb temperature and higher dry bulb temperature, the cooling capacity was greatly influenced by the mass flow rate ratio of water over air.

(3) In this study, the simplified model of Merkel is used to calculate the heat transfer rate in a fill domain. But the experimental supplement for the coefficient of heat and mass transfer in the two-phase flow is carried out to use the model similar to real situation.

Acknowledgements

This work was supported by grant No. 981-1006-041-2 from the Basic Research program of the Korea Science & Engineering Foundation.

References

(1) Walker, W. H., Lewis, W. K., and McAams, W. H., 1923, *Principles of Chemical Engineering*, McGraw-Hill, New York.

(2) Merkel, F., 1926, *Evaporative Cooling*, Zeits Verein deutscher Ingenieure, Vol. 70, pp. 123-128.

(3) Lichtenstein, T., 1943, "Performance & Selection of Mechanical-Draft Cooling Tower", *ASME Transactions*, Vol. 65, No. 7, pp. 779-789.

(4) Baker, D. R. and Shryock, H. A., 1961, "A Comprehensive Approach to the Analysis of Cooling Tower Performance", *ASME J. Heat Transfer*, Vol. 83, pp. 339-349.

(5) Cooling Tower Institute, 1967, *Cooling Tower Performance Curves*, Houston, Texas.

(6) Majumdar, A. K., Singhal, A. K. and Spalding, D. B., 1983, "Numerical Modeling of Wet Cooling Towers - Part 1", *ASME J. Heat Transfer*, Vol. 105, No. 4, pp.

728-735.

(7) Launder, B.E. and Spalding, D.B., 1972, *Mathematical Models of Turbulence*, Academic Press.

(8) Kelly, N.W., 1976, *Kelly's Handbook of Crossflow Cooling Tower Performance*, Neil W. Kelly and Associates, Kansas City, Missouri.

(9) PROPATH group, 1993, *A Program Package for Thermophysical Properties of Fluids*, Version 8.1/MS-DOS, PROPATH group.

(10) Majumdar, A. K., Singhal, A. K., and Spalding, D. B., 1983, "Numerical Modeling of Wet Cooling Towers - Part 2", *ASME J. Heat Transfer*, Vol. 105, No. 4, pp. 728-735.

(11) Zerna, W. and Mungam, I., 1980, "Construction and Design of Large Cooling Towers", *J. The Structural Division.*

(12) Rhie, C.M., 1981, "A Numerical Study of the Flow past an Isolated Airfoil with Separation", *Ph.D. thesis*, Dept. of Mech., University of Illinois Urbana-Champagne.